

# ChemComm

Accepted Manuscript



This is an *Accepted Manuscript*, which has been through the Royal Society of Chemistry peer review process and has been accepted for publication.

*Accepted Manuscripts* are published online shortly after acceptance, before technical editing, formatting and proof reading. Using this free service, authors can make their results available to the community, in citable form, before we publish the edited article. We will replace this *Accepted Manuscript* with the edited and formatted *Advance Article* as soon as it is available.

You can find more information about *Accepted Manuscripts* in the [Information for Authors](#).

Please note that technical editing may introduce minor changes to the text and/or graphics, which may alter content. The journal's standard [Terms & Conditions](#) and the [Ethical guidelines](#) still apply. In no event shall the Royal Society of Chemistry be held responsible for any errors or omissions in this *Accepted Manuscript* or any consequences arising from the use of any information it contains.

## COMMUNICATION

# Selective Disruption of Each Part of Janus Molecular Assemblies by Lateral Diffusion of Stimuli-Responsive Amphiphilic Peptide

Cite this: DOI: 10.1039/x0xx00000x

Received 00th January 2012,  
Accepted 00th January 2012

DOI: 10.1039/x0xx00000x

www.rsc.org/

Motoki Ueda,<sup>a</sup> Akihiro Uesaka<sup>b</sup> and Shunsaku Kimura<sup>b</sup>

**Stimuli-Responsive Janus-type assemblies with a round-bottom flask shape are prepared from amphiphilic helical peptides by the patchwork self-assembly technique. It can disassemble selectively at the neck or the round-bottom part of the Janus assemblies at low pH with heat treatment accompanied by the lateral diffusion of the peptides.**

Janus materials are currently extended to nano-order objects having more than two parts with distinct chemical and physical properties.<sup>1–7</sup> They have gained growing interest for both academic and industrial point of views,<sup>4,6,8–10</sup> because the nano-order object can elicit highly efficient function due to the confinement of several kinds of functional chemical species into different parts of the Janus structure.

One culmination of the Janus materials is a living cell. Cell membranes are phase-separated to concentrate specific proteins and lipids (rafts) for example to realize rational signal transduction through the cell membrane.<sup>11–16</sup> On the other hand, the Janus-type molecular self-assemblies were also prepared by synthetic amphiphiles. One example is DNA-functionalized giant liposome by controlling a mixing ratio of lipid and cholesterol.<sup>17</sup> The DNA components were condensed in a liquid-ordered ( $L_o$ ) phase, which became adhesive to the  $L_o$  phase of different liposomes. The other is UV irradiation-induced disassembly of the nanotube part of the vesicle-capped nanotubes which were prepared from phospholipids and photochemically active amphiphilic molecules with two hydrophobic legs.<sup>18</sup> These Janus-type molecular assemblies are attractive because of simple and easy preparation, a bottom-up process, and controllable dynamics (fluidity and fusion).

We demonstrated previously a Janus-type molecular assembly prepared by phase separation of amphiphilic helical peptides in membrane, which is named “the patchwork self-assembly”.<sup>19</sup> Poly(sarcosine)-*b*-(L-Leu-Aib)<sub>6</sub> (SLL) self-assembled into nanotubes

but into vesicles when mixed with an equimolar amount of poly(sarcosine)-*b*-(D-Leu-Aib)<sub>6</sub> (SDL). When SLL and SDL were mixed at a molar ratio of 2:8 or 8:2, the mixture generated a Janus-type molecular assembly of a round-bottom flask-shaped morphology. The membrane was phase-separated into an equimolar mixture of SLL and SDL and the excessive helical component, which correspond to the round-bottom part and the neck part, respectively, of the Janus-type morphology.

In the present study, a stimuli-responsive Janus-type assembly is studied. The characteristic point of the Janus assembly is coexistence of two or more distinct parts in the assembly. We therefore focused our attention here to introduce the stimuli-responsive molecule selectively into one of the parts. We have prepared the round-bottom flask-shaped assemblies with using SLL, SDL, and a pH-responsive peptide of SHLL, (poly(sarcosine))<sub>3</sub>-*b*-((L-His)<sub>2</sub>-(L-Leu-Aib)<sub>6</sub>) (Fig. 1). Since SHLL contains a His dipeptide at the connection region of the hydrophilic block and the hydrophobic helical block, SHLL is found here to disassemble either one of the neck and the round-bottom parts of the Janus-type assemblies at acidic condition with heat treatment when it is self-assembled into the part. The patchwork assembly technique enables preparations of the round-bottom flask-shaped assemblies containing SHLL selectively either in the neck part or the round-bottom part.

The stereocomplex formation between the right-handed and the left-handed helices is the basis for the formation of the round-bottom flask-shaped assemblies with using SLL, SDL, and SHLL. The concavo-convex interaction between neighboring  $\alpha$ -helical blocks decides precisely the size and shape of the molecular assemblies.<sup>19–23</sup> Further, the amphiphilic helical peptides are allowed to diffuse laterally in the assemblies at high temperatures.<sup>24</sup> With heat treatment, the Janus-type assemblies have the thermodynamically phase-separated membranes. Taking these points into consideration, we have prepared three types of the round-bottom flask-shaped

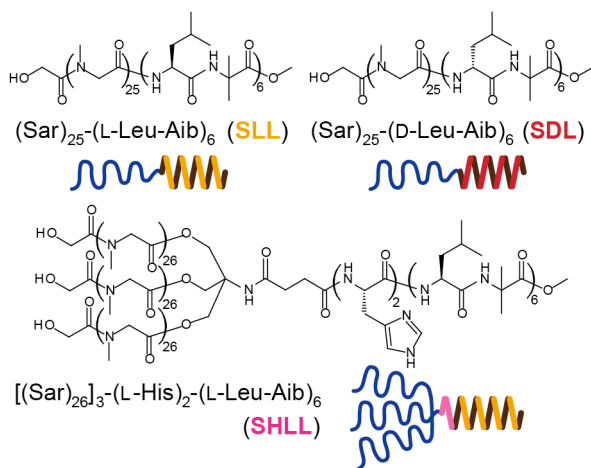


**Fig. 1.** Schematic illustration and chemical structures of amphiphilic polypeptides,  $(\text{Sar})_{25}\text{-}b\text{-}(\text{L-Leu-Aib})_6$  (**SLL**),  $(\text{Sar})_{25}\text{-}b\text{-}(\text{D-Leu-Aib})_6$  (**SDL**) and  $[(\text{Sar})_{26}]_3\text{-}b\text{-}((\text{L-His})_2\text{-}(\text{L-Leu-Aib})_6)$  (**SHLL**).

assemblies, and their stimuli-responsive behaviors were examined.

The  $A_3B$ -type amphiphile with a His dipeptide between the hydrophilic  $A_3$  block and the hydrophobic B block,  $[(\text{Sar})_{26}]_3\text{-}b\text{-}((\text{L-His})_2\text{-}(\text{L-Leu-Aib})_6)$  (**SHLL**) (Fig. 1), formed small curved sheet assemblies upon injection into a Tris buffer at pH 7.4, but the small sheets grew into nanotube assemblies with 50 nm diameter and 100 nm length upon heat treatment (90 °C, 60 min) (Fig. 2a). On the other hand, in our previous report, each of the AB-type amphiphilic polypeptides,  $(\text{Sar})_{25}\text{-}b\text{-}(\text{L-Leu-Aib})_6$  (**SLL**) and  $(\text{Sar})_{25}\text{-}b\text{-}(\text{D-Leu-Aib})_6$  (**SDL**) (Fig. 1), formed large curved sheets in a Tris buffer, and the curved sheets stuck the opposite edges together to form nanotubes with a uniform size of 80 nm diameter and 200 nm length with heat treatment (90 °C, 10 min).<sup>20</sup> In either case, the nanotube sizes were highly homogeneous. We currently consider that the sizes of the curved sheets should be determined by the shielding degree of the hydrophobic edges of the sheets by the hydrophilic block. When the hydrophobic edges are shielded, the growth of the molecular assemblies should be suppressed due to the limited contact of the edges. Since the bulky  $[(\text{Sar})_{26}]_3$  ( $A_3$ ) block of

**SHLL** should be more effective to shield the hydrophobic edge than the  $(\text{Sar})_{25}$  ( $A$ ) block of **SLL** or **SDL**, and therefore the sheet size of **SHLL** became smaller than that of **SLL** or **SDL**. Further, the larger steric hindrance of the  $[(\text{Sar})_{26}]_3$  ( $A_3$ ) block of **SHLL** should favor the larger curvature of the molecular assemblies, resulting in smaller size of the molecular assemblies.

The  $pK_a$  value of the His residues in the **SHLL** assembly was found to be 5.8 by the pH titration analysis (Fig. S1, †ESI). When the **SHLL** nanotubes were prepared at pH 7.4 and the medium was acidified down to pH 5.0, the nanotube morphology was preserved despite of protonation on the His residues. However, with a further heat treatment at 70 °C for 1 h, the irregular tubes and curved sheets in addition to the nanotubes were observed in the TEM images (Fig. 2b). It is therefore considered that the heat treatment in addition to protonation of the His residues are required for the morphology distortion. In order to induce the morphology changes, a heat treatment was required to overcome the activation energy.

A mixture of **SHLL** and **SDL** in ethanol was injected in a Tris buffer at pH 7.4 and treated with heating at 90 °C for 1 h. With this molecular combination of the right-handed helix of **SHLL** and the left-handed helix of **SDL**, the vesicular morphology with *ca.* 120 nm diameter was identified by TEM observation (Fig. 2c and S2a, †ESI). The vesicle formation is in line with the previous report that a mixture of the right-handed helix of **SLL** and the left-handed helix of **SDL** formed vesicles with *ca.* 200 nm diameter.<sup>19,20</sup> The vesicles were prepared from a mixture of **SHLL** and **SDL** at pH 7.4, and the medium was acidified down to pH 5.0. Upon heating at 70 °C for 1 h, the vesicles were disrupted into irregular sheets (Fig. 2d and S2b, †ESI). The heat treatment in addition to the acidification is also required for disruption of the vesicles.

A mixture of **SHLL** nanotubes and planar sheets prepared from a mixture of **SLL** and **SDL** yielded a Janus-type assembly of a round-bottom flask-shaped assembly with heat treatment at 90 °C for 1 h (Fig. 3a–d). This round-bottom flask-shaped assembly is in accordance with the previous report that a mixture of **SLL** and **SDL** at 2:8 or 8:2 molar ratio generated the same type of molecular assembly. One difference between the two round-bottom flask-shaped assemblies is about the diameter of the neck part being 50 nm in the combination of **SHLL**, **SLL**, and **SDL** but 80 nm in the combination of **SLL** and **SDL**. This is because the membrane of the round-bottom flask-shaped assembly is phase-separated, and the neck part is constituted by the excessively mixed helix component, and the round-bottom part is constituted by an equal mixture of the right-handed and the left-handed helices. This explanation is confirmed by the observations that the neck part of 50 nm diameter and the round-bottom part of 200 nm diameter correspond to that of the **SHLL** nanotube and that of the **SLL** + **SDL** vesicle, respectively. We can therefore extend our concept of the patchwork assembly here by showing another Janus-type assembly.<sup>19</sup>

The medium of the round-bottom flask assembly was acidified from 7.4 to 4.7 and heated at 70 °C for 1 h. All the round-bottom flask-shaped assemblies were disrupted to leave vesicles with 200 nm diameter and worm-like sheets (Fig. 3e and S3a, †ESI). The morphology transformation can be explainable as the neck part was composed of **SHLL** and disrupted due to protonation of two His residues and the heat treatment. The round-bottom part was composed of **SLL** and **SDL** and was transformed into vesicular morphology with the heat treatment. A separate experiment showed that the **SLL** + **SDL** vesicle was found to be stable at pH 5 with the heat treatment (Fig. S4, †ESI). The worm-like sheets should be the disrupted part of **SHLL** mixed with a small portion of **SLL** and **SDL**.

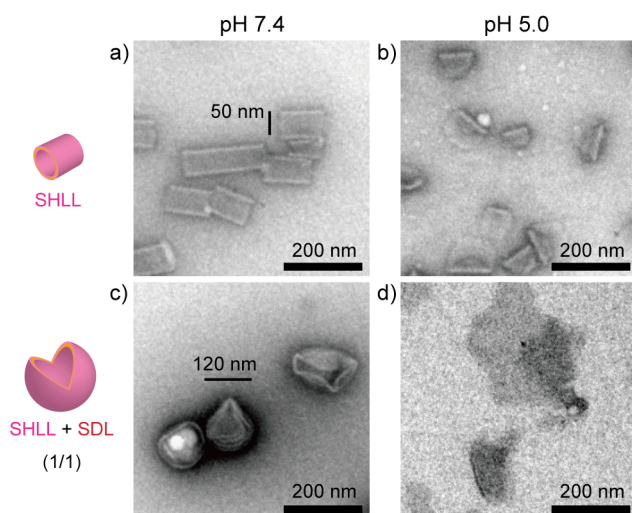


**Fig. 2.** TEM images of molecular assemblies composed of **SHLL** (a, b) and **SHLL** + **SDL** (c, d). The assemblies were prepared in a Tris buffer at pH 7.4 (a, c), and the dispersions were adjusted at pH 5.0 with 0.1N HCl aq. and heated at 70 °C for 1 h (b, d).

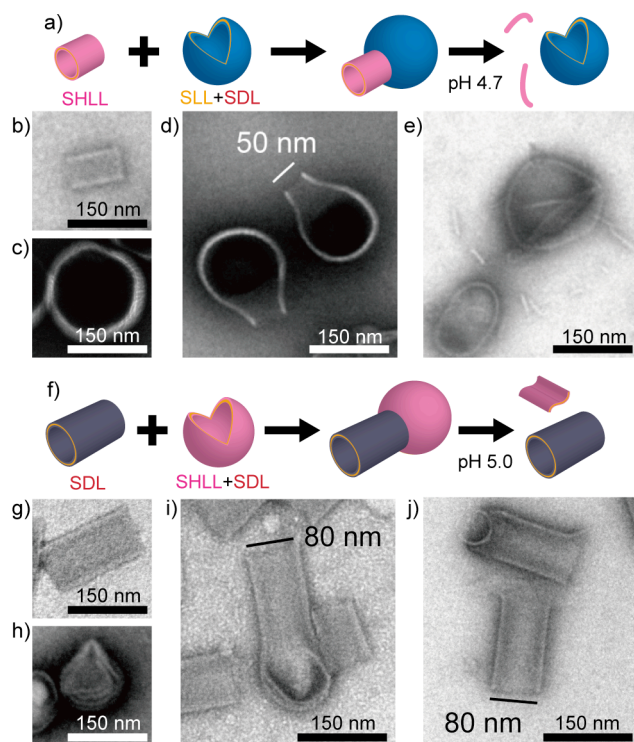


**Fig. 3.** Schematic illustration of stimuli-responsive patchwork assemblies with the stimuli-responsive neck part (a). TEM images of the **SHLL** nanotube (b), the **SLL + SDL** vesicle (c), and the round-bottom flask-shaped assembly (d) in pH 7.4 buffer, and the morphology change after adjusting at pH 4.7 with heat treatment at 70 °C for 1 h (e). Schematic illustration of stimuli-responsive patchwork assemblies with the stimuli-responsive round-bottom part (f). TEM images of the **SDL** nanotube (g), the **SHLL + SDL** vesicle (h), and the round-bottom flask-shaped assembly (i) in pH 7.4 buffer, and the morphology change after adjusting at pH 5.0 with heat treatment at 70 °C for 1 h (j).

Another type of the round-bottom flask-shaped assembly was constructed by a mixture of the **SDL** nanotubes and the **SHLL + SDL** planar sheets with heat treatment at 90 °C for 1 h (Fig. 3f–i). The diameters of the neck part and the round-bottom part were 80 nm and 120 nm, respectively, which shapes and sizes were consistent with those of the **SDL** nanotube and the **SHLL + SDL** vesicle. The patchwork assembly is also successful with the combination of **SHLL** and the excess amount of **SDL**.

When the pH of the medium was decreased down to 5.0 and heated at 70 °C for 1 h, all the round-bottom flask-shaped assemblies were disrupted to leave nanotubes with 80 nm diameter and 180 nm length and irregular small sheets (Fig. 3j and S3b, †ESI). Similarly to the previous explanation for the disruption of the round-bottom flask-shaped assembly of **SHLL**, **SLL**, and **SDL**, the round-bottom part composed of **SHLL** and **SDL** should be disrupted due to the protonation of **SHLL** and the heat treatment, and the neck part of **SDL** was left behind.

In summary, two kinds of the round-bottom flask-shaped assemblies were prepared. In one case of the combination of the **SHLL** nanotube and the **SLL + SDL** vesicle, the neck part of the Janus-type assembly can be selectively disrupted to leave the vesicles. In the other case of the combination of the **SDL** nanotube and the **SHLL + SDL** vesicle, the other round-bottom part of the Janus-type assembly was selectively disrupted. The patchwork assembly is made of the phase-separated membrane, and one part of

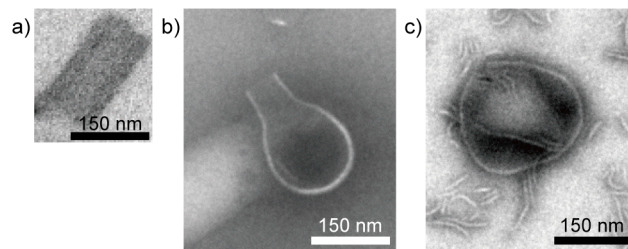


**Fig. 4.** The **SLL** nanotube (a) and the round-bottom flask-shaped assembly prepared from the **SLL** nanotube and the **SHLL + SDL** planar sheets in pH 7.4 buffer (b). The morphology change after adjusting at pH 5.0 with heat treatment at 70 °C for 1 h (c).

the Janus-type assembly can be selectively disrupted by localizing the pH-responsive **SHLL** into those parts. It should be stressed the importance of forming a thermodynamically stable structure of the phase-separated membrane in the Janus-type assembly with heating at 90 °C for 1 h. In these round-bottom flask-shaped assemblies, the peptide membranes were phase-separated into the stereocomplex part of the mixture of the right-handed and the left-handed helices and the other. The thermodynamically stable structure can be obtained only when the lateral diffusions of the amphiphilic helical peptides are allowed in the membrane. In order to confirm the lateral diffusion we examined the following round-bottom flask-shaped assembly. All vesicles, nanotubes and round-bottom flask-shaped assembly kept their morphologies even after further heating at 90 °C for 3 h or cooling at 4 °C for at least 1 week.

When the **SLL** nanotubes and the **SHLL + SDL** planar sheets were mixed and heated at 90 °C for 1 h, the round-bottom flask-shaped assemblies were obtained. When the medium of pH was decreased down to 5.0 and heated at 70 °C for 1 h, all the round-bottom flask-shaped assemblies were disrupted to leave, however, vesicles. The pH-responsive **SHLL** was supposed to be included originally in the round-bottom part, but vesicles were left behind (Fig. 4c and S3c, †ESI). **SHLL** therefore should have diffused out from the round-bottom part to the neck part.

The formation of the round-bottom flask-shaped assembly was studied in detail. When the **SLL** nanotube was mixed with the **SHLL + SDL** planar sheet and heated at 90 °C, the round-bottom flask-shaped assembly was immediately formed (Fig. 4a and 4b). The diameters of the neck part and the round-bottom part were about 80 nm and 120 nm, respectively, suggesting the phase-separation of **SLL** in the neck part and a mixture of **SHLL** and **SDL** in the round-bottom part. However, the dimensions changed with time of heat treatment. The diameter of the neck part decreased to 50 nm as the histogram shows (Fig. 5 and S5, †ESI). Notably, the transient morphology with the thick neck part to the thin one was captured by the TEM image (Fig. 5a). This is a strong evidence for the allowed lateral diffusion of **SHLL** in the phase-separated membrane at 90 °C. At the same time, **SLL** in the neck part should diffuse into the round-bottom part to form the stereocomplex with **SDL** there. As a result, the transient morphology is explainable that the mouth end of the neck part should be rich in **SHLL** to generate the 50 nm nanotube, and the interface end of the neck part with the round-bottom part should be composed of **SLL** left behind to keep the 70–80 nm nanotube.

When a mixture of **SHLL**, **SLL** and **SDL** was injected into a buffer and heated at 90 °C for 1 h, a round-bottom flask-shaped assembly with the 50 nm neck part was observed. It is therefore concluded that the phase separation into the **SHLL** neck part and the **SLL + SDL** round-bottom part is the thermodynamically most stable

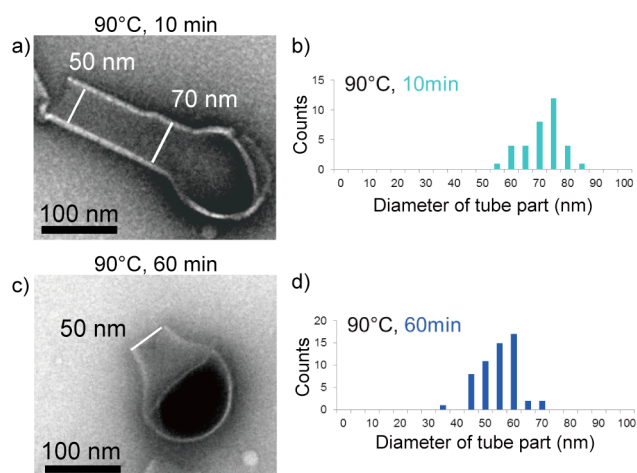


**Fig. 5.** The rearrangement of the component amphiphilic peptides in the round-bottom flask-shaped assembly prepared from the **SLL** nanotube and the **SHLL** + **SDL** sheets with heat treatment. TEM images (a, c) and histograms (b, d) of the round-bottom flask-shaped assemblies with heat treatment at 90 °C for 10 min (a, b) and 60 min (c, d).

in the combination of **SHLL**, **SLL** and **SDL**. The round-bottom flask-shaped assembly with the **SLL** neck part and the **SHLL** + **SDL** round bottom part appeared transiently just after mixing the **SLL** nanotubes and the **SHLL** + **SDL** planar sheets. This transient morphology is therefore kinetically generated. With heating at 90 °C, the amphiphilic helical peptides could diffuse in the membrane to reach the thermodynamically stable phase-separated membrane.

The helical molecules are found to be more tightly packed in the stereocomplex between the right-handed and the left-handed helices than in the pure isomer. The excess helix component should be squeezed out from the stereocomplex part to take the nanotube morphology as the neck part of the round-bottom flask-shaped assembly. The mixture of **SHLL**, **SLL** and **SDL** generated the **SLL** + **SDL** round-bottom part. The **SHLL** + **SDL** round bottom part appeared transiently when the **SHLL** + **SDL** sheets were prepared in advance to mix with the **SLL** nanotubes. Further, **SHLL** diffused out from the **SHLL** + **SDL** round bottom part through the **SLL** neck part. It is therefore suggested that the membrane stability decreases in the order of **SLL**+**SDL** > **SHLL** + **SDL** > **SLL** > **SHLL**. We have examined here the hydrophobic helical blocks only of (L-Leu-Aib)<sub>6</sub> and (D-Leu-Aib)<sub>6</sub>. Other kinds of helical blocks will show different behaviors about the molecular packing, which will make the patchwork assembly more rich in variety.

## Conclusions

The pH-sensitive molecule, **SHLL**, can be confined selectively into one part of the Janus-type assembly of the round-bottom flask-shaped assembly with a suitable combination of other amphiphilic helical peptides. The part containing **SHLL** can be selectively disrupted by acidification and heat treatment with leaving the other part of the Janus-type assembly behind. The Janus-type assembly is attained due to the phase separation in the membrane, and the component amphiphilic peptides can diffuse laterally to reach a thermodynamically stable phase-separated membranes upon heating. These peptides associate together via helix-helix interaction similarly to the Leu-zipper

motif to some extent. There are a lot of variations about the helix-helix interaction in nature, which can be applied to the patchwork assemblies to make them valuable peptide materials.

## Notes and references

<sup>a</sup> Clinical Division of Diagnostic Radiology, Kyoto University Hospital 54 Shogoin Kawara-cho, Sakyo-ku, Kyoto, 606-8507, Japan.

<sup>b</sup> Department of Material Chemistry, Graduate School of Engineering, Kyoto University Kyoto-Daigaku-Katsura, Nishikyo-ku, Kyoto, 615-8510, Japan

† Electronic Supplementary Information (ESI) available: [details of any supplementary information available should be included here]. See DOI: 10.1039/c000000x/

- 1 Perro, A.; Reculusa, S.; Ravaine, S.; Bourgeat-Lami, E.; Duguet, E. *J. Mater. Chem.* **2005**, *15*, 3745–3760.
- 2 Walther, A.; Müller, A. H. E. *Chem. Rev.* **2013**, *113*, 5194–5261.
- 3 Seo, K. D.; Doh, J.; Kim, D. S. *Langmuir* **2013**, *29*, 15137–15141.
- 4 Sacanna, S.; Korpics, M.; Rodriguez, K.; Colón-Meléndez, L.; Kim, S.-H.; Pine, D. J.; Yi, G.-R. *Nat. Commun.* **2013**, *4*, 1688.
- 5 Kaufmann, T.; Gokmen, M. T.; Rinnen, S.; Arlinghaus, H. F.; Prez, F. D.; Ravoo, B. J. *J. Mater. Chem.* **2012**, *22*, 6190–6199.
- 6 Roh, K.-H.; Martin, D. C.; Lahann, J. *Nat. Mater.* **2005**, *4*, 759–763.
- 7 Liu, Y.; Li, Y.; He, J.; Duelle, K. J.; Lu, Z.; Nie, Z. *J. Am. Chem. Soc.* **2014**, *136*, 2602–2610.
- 8 Yan, J.; Chaudhary, K.; Chul Bae, S.; Lewis, J. A.; Granick, S. *Nat. Commun.* **2013**, *4*, 1516.
- 9 Bhaskar, S.; Gibson, C. T.; Yoshida, M.; Nandivada, H.; Deng, X.; Voelcker, N. H.; Lahann, J. *Small* **2011**, *7*, 812–819.
- 10 Nisisako, T.; Torii, T.; Takahashi, T.; Takizawa, Y. *Adv. Mater.* **2006**, *18*, 1152–1156.
- 11 Simons, K.; Ikonen, E. *Nature* **1997**, *387*, 569–572.
- 12 Brown, D. A.; London, E. *J. Biol. Chem.* **2000**, *275*, 17221–17224.
- 13 Simons, K.; Toomre, D. *Nat. Rev. Mol. Cell Biol.* **2000**, *1*, 31–39.
- 14 Anderson, R. G. W.; Jacobson, K. *Science* **2002**, *296*, 1821–1825.
- 15 Lingwood, D.; Simons, K. *Science* **2010**, *327*, 46–50.
- 16 Head, B. P.; Patel, H. H.; Insel, P. A. *Biochim. Biophys. Acta BBA - Biomembr.* **2014**, *1838*, 532–545.
- 17 Beales, P. A.; Nam, J.; Vanderlick, T. K. *Soft Matter* **2011**, *7*, 1747–1755.
- 18 Coleman, A. C.; Beierle, J. M.; Stuart, M. C. A.; Maciá, B.; Caroli, G.; Mika, J. T.; van Dijken, D. J.; Chen, J.; Browne, W. R.; Feringa, B. L. *Nat. Nanotechnol.* **2011**, *6*, 547–552.
- 19 Ueda, M.; Makino, A.; Imai, T.; Sugiyama, J.; Kimura, S. *Polym. J.* **2013**, *45*, 509–515.
- 20 Ueda, M.; Makino, A.; Imai, T.; Sugiyama, J.; Kimura, S. *Chem. Commun.* **2011**, *47*, 3204–3206.
- 21 Uesaka, A.; Ueda, M.; Imai, T.; Sugiyama, J.; Kimura, S. *Langmuir* **2014**, *30*, 4273–4279.
- 22 Uesaka, A.; Ueda, M.; Makino, A.; Imai, T.; Sugiyama, J.; Kimura, S. *Langmuir* **2014**, *30*, 1022–1028.
- 23 Ueda, M.; Makino, A.; Imai, T.; Sugiyama, J.; Kimura, S. *J. Pept. Sci.* **2011**, *17*, 94–99.
- 24 Ueda, M.; Makino, A.; Imai, T.; Sugiyama, J.; Kimura, S. *Langmuir* **2011**, *27*, 4300–4304.